Control Engineering Practice 18 (2010) 318–329

Contents lists available at ScienceDirect

Control Engineering Practice

journal homepage: www.elsevier.com/locate/conengprac

A linear-interpolation-based controller design for trajectory tracking of mobile robots

Gustavo Scaglia [a,b,*], Andrés Rosales [b], Lucia Quintero [b], Vicente Mut [b], Ravi Agarwal [c]

[a] Instituto de Ingeniería Química, Universidad Nacional de San Juan, Argentina
[b] Instituto de Automática, Universidad Nacional de San Juan, Argentina
[c] Department of Mathematics, Florida Institute of Technology, USA

ARTICLE INFO

Article history:
Received 26 August 2008
Accepted 20 November 2009
Available online 23 December 2009

Keywords:
Control system design
Nonlinear model
Tracking trajectory control
Mobile robot
Numerical methods

ABSTRACT

This work presents a novel linear interpolation based methodology to design control algorithms for the trajectory tracking of mobile robotic systems. Particularly, a typical nonlinear multivariable system—a mobile robot—is analysed. The methodology is simple and can be applied to the design of a large class of control systems. Simulation and experimental results are presented and discussed, demonstrating the good performance of the proposed methodology.

1. Introduction

One of the main problems found in mobile robot control is trajectory tracking. In general, the objective is that the mobile robot can reach a prescribed Cartesian position (x, y) with a pre-established orientation θ for each sampling period. These combined actions result in tracking some desired trajectory of the mobile robot. In order to achieve this objective, commonly two control variables are available, namely: robot's linear velocity V and the angular velocity W.

The use of trajectory tracking for a navigation system is justified in structured workspaces as well as in partially structured workspaces, where unexpected obstacles can be found during the navigation. In the first case, the reference trajectory can be set from a global trajectory planner. In the second case, the algorithms used to avoid obstacles usually re-plan the trajectory in order to avoid a collision, generating a new reference trajectory from this point on. Besides, there exist algorithms that express the reference trajectory of the mobile robot as function of a descriptor called r (Del Rio, Jiménez, Sevillano, Amaya, & Balcells, 2002) or s (called "*virtual time*") (Lee & Park, 2003) whose derivative is a function of the tracking error and the time t. For example, if the tracking error is large, the reference trajectory should wait for the mobile robot; otherwise, if the tracking error is small, then the reference trajectory must tend to the original trajectory calculated by the global planner. In this way, the module of trajectory tracking will use the original path or the on-line recalculated path as reference to obtain the smallest error when the mobile robot follows the path (Normey-Rico, Gomez-Ortega, & Camacho, 1999). Therefore, the trajectory tracking is always important independently from whether the reference trajectory has been generated by a trajectory global planner or a local one.

Various control strategies have been proposed for trajectory tracking, some of which are based on either kinematic or dynamic models of the mobile robot (Lee, Song, Lee, & Teng, 2001), depending on the operative speed and the precision of the dynamic model, respectively (Do & Pan, 2006). Different structures to control these systems have been developed as well. In Tsuji, Morasso, and Kaneko (1995), the authors used a time-varying feedback gain whose evolution can be modified through parameters that determine the convergence time and the behaviour of the system. In Fierro and Lewis (1995), the controller proposed by Kanayama, Kimura, Miyazaki, and Noguchi (1990) is used to generate the inputs to a velocity controller, making the position error asymptotically stable. So, a controller to force the velocity of the mobile robot to follow the reference velocity is designed. The work of Fukao, Nakagawa, and Adachi (2000), extends the design proposed by Fierro and Lewis (1995) and considers that the model parameters are unknown. In Kim, Shin, and Lee (2000), an adaptive controller that takes into account the parametric uncertainties and the robot external perturbations to guarantee perfect velocity tracking is proposed. The reference

* Corresponding author at: Instituto de Ingeniería Química, Universidad Nacional de San Juan, Argentina. Tel.: +54 264 421 3303; fax: +54 264 421 3672.
E-mail addresses: gscaglia@unsj.edu.ar (G. Scaglia), arosales@inaut.unsj.edu.ar (A. Rosales), olquinte@inaut.unsj.edu.ar (L. Quintero), vmut@inaut.unsj.edu.ar (V. Mut), agarwal@fit.edu (R. Agarwal).

0967-0661/$ - see front matter © 2009 Elsevier Ltd. All rights reserved.
doi:10.1016/j.conengprac.2009.11.011

velocity is obtained by using the controller proposed by Kanayama et al. (1990). In Chwa (2004) two controllers are designed; they are called position controller and heading controller. The former ensures position tracking and the latter is activated when tracking error is little enough and tracking reference does not change its position. This reduces the error over the mobile robot orientation at the end of the path. In Shim and Sung (2004) the posture controller is designed in function of posture error and, in this way, the reference velocities are generated on the basis of a specification set as: (i) if the distance to a reference posture is relatively large, then the robot movement is quick, and the speed is reduced as the robot approaches to the target; (ii) the robot should take the shortest amount of time to reach the desired posture. Later, the reference velocities input a PID controller that generates the torque needed by the desired speed. In Sun and Cui (2004), a controller for trajectory tracking is designed using the kinematic model of the mobile robot and a transformation matrix. Such matrix is singular if the linear velocity of the mobile robot is zero. Therefore, the effectiveness of that controller is ensured only if the velocity is different from zero. Simulation results using linear velocity different from zero as initial condition are shown in that paper. In Sun (2005) a controller based on the error model of Kanayama et al. (1990) is proposed. This controller is formed by two equations which are switched depending on the value of the angular velocity of the mobile robot and the prescribed tolerance of it. In Martins, Celeste, Carelli, Sarcinelli-Filho, and Bastos-Filho (2008) an adaptive controller used to guide a mobile robot during trajectory tracking is proposed. Initially, the desired values of the linear and angular velocities are generated, considering only the kinematic model of the robot. Next, such values are processed to compensate the robot dynamics, thus generating the commands of linear and angular velocities delivered to the robot actuators.

The trajectory tracking for mobile robots is characteristically a nonlinear problem. Diverse model-based classic techniques, which propose controllers with a zero-error tracking, have been applied to solve this problem. However, these classic approaches involve an online matrix inversion (e.g. Klanèar & Škrjank, 2007; Vougioukas, 2007), which represents a drawback in the implementation of the aforementioned methods. In this paper, the proposed algorithm does not involve online matrix inversion problems. Most surveys do not present a final expression for the control signals of their controllers (e.g. Liu, Jing, Ding, & Li, 2008; Tsai, Wang, Chang, & Wu, 2004; Wang & Tsai, 2004), because the computation of these control variables must be made by using demanding computer operations. On the other hand, some current straightforward methods present just simulations (Dong & Guo, 2005; Liu, Zhang, Yang, & Yu, 2004; Zhang, Dai, & Zeng, 2007). In this paper, the design of the proposed control law by using linear algebra tools and furthermore the final expression for the control signals, which will be directly implemented on the mobile robot, are presented.

In this paper, a simple approach to track trajectories is proposed. To achieve this goal, it is assumed that the evolution of the system can be approximated by a linear interpolation in each sampling time. Under this assumption, and knowing the desired state, a value for the control action needed to force the system to go from its current state to a desired one can be obtained. As it is a linear approximation, clearly, the tracking errors can be reduced by decreasing the sampling time. The main contribution of this work is that the proposed methodology is based upon easily understandable concepts, and that there is no need for complex calculations to attain the control signal. In this work the control schemes presented in Fierro and Lewis (1995), Fukao, Nakagawa, and Adachi (2000), Kim et al. (2000), Shim and Sung (2004), Cruz, Mcclintock, Perteet, Orqueda, and Cao (2007) will be employed. Accordingly, a kinematic controller is designed first, which generates the reference velocity in order to reach the desired goal. Additionally, this reference is employed to input a velocity controller in the scheme. In our work a PID controller is used as a velocity controller. The implemented controller will be placed on board an existing mobile robot in order to maintain its translational and rotational speeds at desired values (Cruz et al., 2007; Shim & Sung, 2004). In general, most market-available robots have low level PID velocity controllers to track input reference velocities and do not allow the motor voltage to be driven directly. Therefore, it is useful to express the mobile robot model in a suitable way by considering rotational and translational reference velocities as control signals. Furthermore, the velocity controller follows asymptotically its references.

Besides, in this work it is not necessary to switch the controller as in Chwa (2004) in cases when position reference does not change and tracking error is small. The purpose of this paper is that when this situation is detected, the desired orientation changes, calculating the control signal by using the same expression. Additionally, this approach does not suffer from the disadvantage of the controller by Sun & Cui (2004), where a linear velocity different from zero is necessary for good working. Furthermore, this controller does not need to change the control expression when the angular velocity is lower than a pre-established value in contrast to Sun (2005). In addition, Scaglia, Quintero, Mut, and di Sciascio (2008) introduce a numerical methods based controller, where the control law depends on the chosen numerical approximation. In the current work, very-low tracking errors are obtained, taking into account that linear and angular velocities are not considered during the controller design. Besides, a proof of the zero-convergence of the tracking error is also included.

The paper is organized as follows: Section 2 presents the methodology for the controller design using a linear interpolation method and describes the application of the methodology to a multi-variable nonlinear system. This is illustrated in a case study involving a mobile robot PIONEER 2DX. Afterwards, the formulation of the proposed control algorithm is obtained. In Section 3 the results and a further discussion about the tracking, positioning and the movement of the mobile robot into a real environment are presented. Conclusions are detailed in Section 4 and finally, Appendix A refers the demonstration of the error tendency to zero.

2. Methodology for controller design for a mobile robot

Linear interpolation is the basis for many numerical methods. Let us consider Fig. 1 and a smooth nonlinear function $y=g(x)$ in the interval $[a, b]$ then, a linear interpolation is valid:

$$P(x)=\frac{g(b)-g(a)}{b-a}(x-a)+g(a) \tag{1}$$

The interpolation error $e(x)=g(x)-P(x)$ is bounded and it is valid

$$|e(x)|\leq\tfrac{1}{2}|(x-a)(x-b)|\max_{a\leq x\leq b}|g''(x)| \tag{2}$$

Based on the continuity and smoothness of $g(x)$ and assuming a sufficiently small interval $[a, b]$, one gets that the maximum of $g''(x)$ occurs approximately at the middle point $x_m=0.5(a+b)$, and if the second derivative remains approximately constant in the interval, then it can be approximated by $g''(x_m)$. In this paper, these results will be used to obtain the control for reference tracking. The methodology used will be described next. Let us

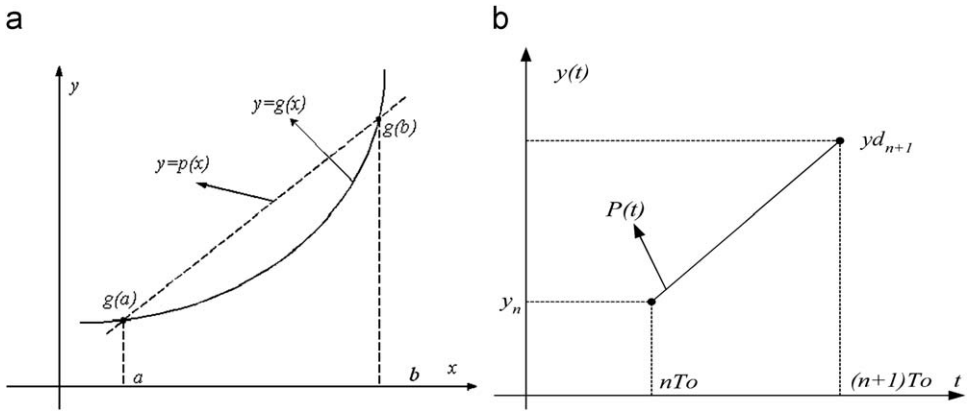

Fig. 1. (a) Linear interpolation. (b) Approximation of the evolution of $y(t)$ in the interval $[nTo\ (n+1)To]$.

consider the first-order differential equation

$$\frac{dy}{dt} = \dot{y} = f(y,t,u), \quad y(0) = yo \tag{3}$$

where y represents the system output, u the control action, and t the time. The values of $y(t)$ at discrete time $t = nTo$, where To is the sampling period, which comes from the length of $[a,\ b]$, and $n \in \{0,1,2,3,\ldots\}$ will be denoted as y_n. The value of y_{n+1} is

$$y_{n+1} = y_n + \int_{nTo}^{(n+1)To} f(y,t,u)\,dt \tag{4}$$

where u remains constant during the interval $nTo \le t < (n+1)To$. Therefore, if one knows beforehand the desired trajectory (referred to as $yd(t)$) to be followed by $y(t)$, then y_{n+1} can be substituted by yd_{n+1} into (4) and considering that the system is evolving according to the linear approximation $P(t)$ (see Fig. 1b, Eq. (1)), then it is possible to calculate u_n that represents the control action required to go from the current state to the desired one. If $P(t)$ is defined as a system trajectory from the current position to the desired one in the next sample time, and using a linear interpolation, it is obtained

$$P(t) = y_n + \frac{yd_{n+1} - y_n}{To}(t - nTo) \tag{5}$$

This will help to calculate the control action required to reach the desired value, substituting (5) into (4), it yields

$$y_{n+1} \approx y_n + \int_{nTo}^{(n+1)To} f(P(t),t,u)\,dt \tag{6}$$

Finally, (6) can be solved for u, in such a way that the distance between the current state and the desired one results minimal.

Next, the approximation described in (6) is applied to a multivariable nonlinear model of a nonholonomic mobile robot (see (11)). This nonlinear multivariable model (Fig. 2a) is given by

$$\begin{cases} \dot{x} = V\cos\theta \\ \dot{y} = V\sin\theta \\ \dot{\theta} = W \end{cases} \tag{7}$$

where V and W are the linear and angular velocities of the mobile robot, respectively, (x,y) is the Cartesian position, and θ is the orientation of the mobile robot(Campion, Bastin, & d'Andrea-Novel, 1996; Secchi, 1998).

Then, the aim of this work is to find the values of V and W, so that the mobile robot can follow a pre-established trajectory.

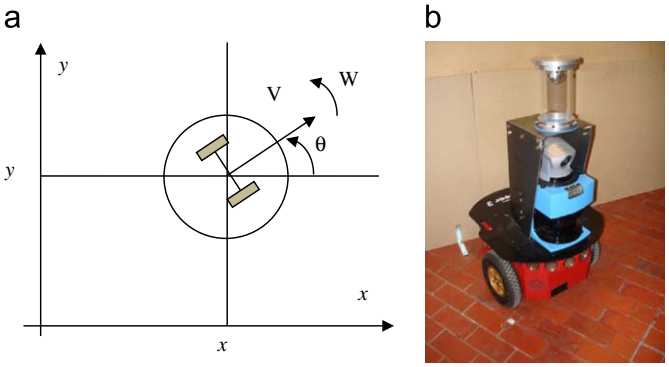

Fig. 2. (a) Geometric description of the mobile robot. (b) Pioneer 2DX mobile robots and its environment.

Moreover, the reference trajectory fulfills:

$$\begin{cases} \dot{x}\,ref = Vref\cos\theta\,ref \\ \dot{y}\,ref = Vref\sin\theta\,ref \\ \dot{\theta}\,ref = Wref \end{cases} \tag{8}$$

where $Vref$ and $Wref$ are the linear and angular velocities, respectively, used to generate the reference trajectory to be followed by the mobile robot. The variables $xref(t)$, $yref(t)$ and $\theta ref(t)$ are the positions and orientation that composed the reference trajectory.

From (4) and (7), it follows:

$$\begin{cases} x_{n+1} = x_n + \int_{nTo}^{(n+1)To} V\cos\theta\,dt \\ y_{n+1} = y_n + \int_{nTo}^{(n+1)To} V\sin\theta\,dt \\ \theta_{n+1} = \theta_n + \int_{nTo}^{(n+1)To} W\,dt \end{cases} \tag{9}$$

where V and W remain constant in the interval $nTo \le t < (n+1)To$ and equal to V_n and W_n. The consideration that linear and angular velocities are kept constant during each sampling time with discontinuities for each nTo is not real, because linear and angular velocities of any mobile robot change continually with the time. By using this approximation, it is assumed that the evolution of the state variables, during each sampling time, follows a tendency represented by a linear interpolation. Then, for $t \in [nTo, (n+1)To]$, it is valid

$$\begin{cases} \theta(t) = \theta_n + W_n(t - nTo) \\ \theta_{n+1} = \theta_n + W_n To \end{cases} \tag{10}$$

Substituting (10) into (9), x can be represented

$$x_{n+1} = x_n + V_n \int_{nTo}^{(n+1)To} \cos[\theta_n + W_n(t-nTo)]\,dt \tag{11}$$

where

$$\int_{nTo}^{(n+1)To} \cos[\theta_n + W_n(t-nTo)]\,dt = \frac{1}{W_n}\{\sin\theta_{n+1} - \sin\theta_n\} \tag{12}$$

From (11) and (12) one gets

$$x_{n+1} = x_n + V_n \frac{1}{W_n}\{\sin\theta_{n+1} - \sin\theta_n\} \tag{13}$$

Analogously for y

$$y_{n+1} = y_n + V_n \frac{1}{W_n}\{\cos\theta_n - \cos\theta_{n+1}\} \tag{14}$$

Finally, in vector form one attains

$$\begin{bmatrix} x_{n+1} \\ y_{n+1} \\ \theta_{n+1} \end{bmatrix} = \begin{bmatrix} x_n \\ y_n \\ \theta_n \end{bmatrix} + \begin{bmatrix} \frac{1}{W_n}\{\sin\theta_{n+1} - \sin\theta_n\} & 0 \\ \frac{1}{W_n}\{\cos\theta_n - \cos\theta_{n+1}\} & 0 \\ 0 & To \end{bmatrix} \begin{bmatrix} V_n \\ W_n \end{bmatrix} \tag{15}$$

Remark. Eq. (15) remains bounded when $W_n \to 0$. The expresion for x_{n+1} is analized

from (10) and (13):

$$x_{n+1} = x_n + V_n \frac{1}{W_n}\{\sin\theta_{n+1} - \sin\theta_n\} = x_n + V_n \frac{To}{\theta_{n+1} - \theta_n}\{\sin\theta_{n+1} - \sin\theta_n\}$$

then, if $W_n \to 0$

$$\lim_{W_n \to 0} \frac{1}{W_n}\{\sin\theta_{n+1} - \sin\theta_n\} = \lim_{(\theta_{n+1} - \theta_n) \to 0} To \frac{\sin\theta_{n+1} - \sin\theta_n}{\theta_{n+1} - \theta_n} = To\cos\theta_n$$

Note that when $W_n \to 0$ the term $1/W_n\{\sin\theta_{n+1} - \sin\theta_n\}$ remains bounded, in a similar way it is demonstrable that the term $1/W_n\{\cos\theta_n - \cos\theta_{n+1}\}$ also remains bounded.

As the desired vector $[xd_{n+1}\ yd_{n+1}\ \theta d_{n+1}]^T$ is known beforehand, it can substitute this in the left hand of (15) instead of $[x_{n+1}\ y_{n+1}\ \theta_{n+1}]^T$ in order to calculate the control signals V_n, W_n necessary for to the trajectory tracking. Let $\Delta x = xd_{n+1} - x_n, \Delta y = yd_{n+1} - y_n, \Delta\theta = \theta d_{n+1} - \theta_n$, then, from (15)

$$W_n = \frac{\theta d_{n+1} - \theta_n}{To} = \frac{\Delta\theta}{To} \tag{16}$$

$$\begin{bmatrix} \Delta x \\ \Delta y \end{bmatrix} = \begin{bmatrix} xd_{n+1} - x_n \\ yd_{n+1} - y_n \end{bmatrix}, A = \begin{bmatrix} \frac{1}{\left(\frac{\theta_{n+1} - \theta_n}{To}\right)}\{\sin\theta_{n+1} - \sin\theta_n\} \\ \frac{1}{\left(\frac{\theta_{n+1} - \theta_n}{To}\right)}\{\cos\theta_n - \cos\theta_{n+1}\} \end{bmatrix}$$

$$\Rightarrow A \underbrace{V_n}_{x} = \underbrace{\begin{bmatrix} \Delta x \\ \Delta y \end{bmatrix}}_{b} \tag{17}$$

Eq. (17) is a system of two equations with a single unknown, that is $Ax = b$, whose optimal solution by minimal square is (Strang, 1980)

$$A^T A V_n = A^T b \tag{18}$$

with

$$V_n = \frac{(\theta_{n+1} - \theta_n)}{(\sin\theta_{n+1} - \sin\theta_n)^2 + (\cos\theta_n - \cos\theta_{n+1})^2}\left[\frac{\Delta x}{To}(\sin\theta_{n+1} - \sin\theta_n) + \frac{\Delta y}{To}(\cos\theta_n - \cos\theta_{n+1})\right] \tag{19}$$

In general, the equation system (17) has no solution and (19) represents an approximate one, according to least squares of (17). So that, (17) has an exact solution, the term b must belong to the column space of A (CSA), where CSA is defined by

$$CSA = \left\{ \begin{bmatrix} x1 \\ x2 \end{bmatrix} \Big/ \begin{bmatrix} x1 \\ x2 \end{bmatrix} = kA, k \in \Re \right\}$$

$\Re$ field of real number. A base of CSA (B(CSA)) is given by

$$B(CSA) = \{v\} = \left\{ \begin{bmatrix} \sin\theta_{n+1} - \sin\theta_n \\ \cos\theta_n - \cos\theta_{n+1} \end{bmatrix} \times \frac{1}{\sqrt{(\sin\theta_{n+1} - \sin\theta_n)^2 + (\cos\theta_n - \cos\theta_{n+1})^2}} \right\}$$

The component of b in the column space of A (b_{ECA}) is

$$b_{ECA} = (b^T v)v = \frac{\Delta x(\sin\theta_{n+1} - \sin\theta_n) + \Delta y(\cos\theta_n - \cos\theta_{n+1})}{(\sin\theta_{n+1} - \sin\theta_n)^2 + (\cos\theta_n - \cos\theta_{n+1})^2} \times \begin{bmatrix} \sin\theta_{n+1} - \sin\theta_n \\ \cos\theta_n - \cos\theta_{n+1} \end{bmatrix} \tag{20}$$

So that (17) has an exact solution the condition $b = b_{ECA}$ has to be fulfilled, that is

$$\frac{\Delta x(\sin\theta_{n+1} - \sin\theta_n) + \Delta y(\cos\theta_n - \cos\theta_{n+1})}{(\sin\theta_{n+1} - \sin\theta_n)^2 + (\cos\theta_n - \cos\theta_{n+1})^2} \begin{bmatrix} \sin\theta_{n+1} - \sin\theta_n \\ \cos\theta_n - \cos\theta_{n+1} \end{bmatrix} = \begin{bmatrix} \Delta x \\ \Delta y \end{bmatrix} \tag{21}$$

$$\Delta x(\sin\theta_{n+1} - \sin\theta_n)^2 + \Delta y(\cos\theta_n - \cos\theta_{n+1})(\sin\theta_{n+1} - \sin\theta_n) = \Delta x[(\sin\theta_{n+1} - \sin\theta_n)^2 + (\cos\theta_n - \cos\theta_{n+1})^2]$$

$$\Delta y(\sin\theta_{n+1} - \sin\theta_n) = \Delta x(\cos\theta_n - \cos\theta_{n+1})$$

$$\frac{\sin\theta_{n+1} - \sin\theta_n}{\cos\theta_n - \cos\theta_{n+1}} = \frac{\Delta x}{\Delta y} \tag{22}$$

The value of θ_{n+1} that satisfies (22), will be denominated θez_{n+1} and represents the necessary mobile robot orientation, so that (17) has an exact solution. From (15) θez_{n+1} must satisfy

$$\begin{cases} \sin\theta ez_{n+1} = \frac{W_n}{V_n}\Delta x + \sin\theta_n \\ \cos\theta ez_{n+1} = -\frac{W_n}{V_n}\Delta y + \cos\theta_n \end{cases}$$

If both members are squared and an addition is made, we have

$$(\sin\theta ez_{n+1})^2 + (\cos\theta ez_{n+1})^2 = \left(\frac{W_n}{V_n}\Delta x\right)^2 + 2\frac{W_n}{V_n}\Delta x\sin\theta_n + (\sin\theta_n)^2 + \left(\frac{W_n}{V_n}\Delta y\right)^2 + 2\frac{W_n}{V_n}\Delta y\cos\theta_n + (\cos\theta_n)^2$$

$$\frac{W_n}{V_n}\left\{\frac{W_n}{V_n}\Delta x^2 + 2\Delta x\sin\theta_n + \frac{W_n}{V_n}\Delta y^2 + 2\Delta y\cos\theta_n\right\} = 0$$

$$\frac{W_n}{V_n} = \frac{2(\Delta y\cos\theta_n - \Delta x\sin\theta_n)}{\Delta x^2 + \Delta y^2}$$

$$\theta ez_{n+1} = a\tan\frac{\frac{W_n}{V_n}\Delta x + \sin\theta_n}{-\frac{W_n}{V_n}\Delta y + \cos\theta_n} \tag{23}$$

It can be noticed that (23) fulfills (22).

The x and y errors are defined as $ex_n = xref_n - x_n$, $y_n = yref_n - y_n$. For the error to tend to zero (see Appendix A), we define

$$xd_{n+1} = xref_{n+1} - kx\underbrace{(xref_n - x_n)}_{ex_n}$$

$$yd_{n+1} = yref_{n+1} - ky\underbrace{(yref_n - y_n)}_{ey_n} \tag{24}$$

where kx and ky satisfy $0 < kx,\ ky < 1$.

Consistently, an expression for the desired value of orientation θd_{n+1} to reach null tracking error:

$$\theta d_{n+1} = \theta ez_{n+1} - k\theta\underbrace{(\theta ez_n - \theta_n)}_{e\theta_n} \tag{25}$$

where $k\theta$ satisfy $0 < k\theta < 1$ and θez, which represents the desired orientation that enables the position error to tend to zero.

From (16), (19), (23)–(25) the proposed controller for the mobile robot is given as

$$\begin{bmatrix} V_n \\ W_n \end{bmatrix} = \begin{bmatrix} \frac{(\theta ez_{n+1} - \theta_n)}{a^2 + b^2}\left[\frac{\Delta x}{To}a + \frac{\Delta y}{To}b\right] \\ \frac{\Delta\theta}{To} \end{bmatrix} \tag{26}$$

with, $a = (\sin\theta ez_{n+1} - \sin\theta_n)$ and $b = (\cos\theta_n - \cos\theta ez_{n+1})$.

3. Simulation and experimental results

Simulation and experimental studies were carried out with a mobile robot PIONEER 2DX available at the Instituto de Automática (INAUT) to test the proposed controller performance. Fig. 2b shows the Pioneer 2DX and the laboratory facilities where the experiences were carried out. In the PIONEER 2DX a value of 0.1 s was chosen for the sample time To.

In order to test the performance of the proposed controller, a circumference of 1000 mm radius was used as the desired trajectory, with centre on the origin of the coordinate system. The starting point for the robot was the centre of the circumference, and an initial orientation was $\theta = 0$. From this starting point it evolves to the desired trajectory. The reference trajectory starts at $(1000, 0)$ mm and it is generated at constant linear and angular velocities, respectively, known as $Vref$ and $Wref$. During the execution of the reference trajectory, at a random instant of time, certain values of ($xref$, $yref$) will be kept fixed. In this way, the proposed controller performance is monitored when a trajectory is followed by the mobile robot and then it is suddenly stopped at a certain point.

It is important to remark that the absolute value of the difference between the desired and real trajectory, once the mobile robot has reached the geometric pre-defined trajectory, will be called *error*:

$$Error = \|e_n\| = \sqrt{(ex_n)^2 + (ey_n)^2} \tag{27}$$

Fig. 3 shows the simulation results, where the mobile robot is described by (7). Fig. 3a shows that the mobile robot tends to the reference trajectory and the error tends to zero as shown in Fig. 3b. Fig. 3b presents the time-evolution of the tracking error.

Fig. 4a shows the trajectory followed by the mobile robot in the laboratory on the x–y plane when $Vref = 700$ mm/s, it can be noted that the mobile robot reaches the desired trajectory very quickly, and it follows this trajectory with an error smaller than 50 mm. It may be seen that the robot follows the desired trajectory without oscillations. And in Fig. 4b, the errors for different reference velocities are shown; it can be noted that the maximum tracking error at $Vref$=100 mm/s is 10 mm and for $Vref$=700 mm/s is 45 mm all this error values are small compared with the distance between the axes of the PIONEER 2DX mobile robot, i.e. 330 mm. If Figs. 3b and 4b are compared, the following aspects can be noticed: The tracking error, shown in Fig. 4b, does not tend to zero since (7) represents approximately the mobile robot; also, the tracking error increases as the mobile robot speed is higher due to the dynamic effects of the velocity rise. However, this error remains too low compared with the mobile robot dimensions.

From Figs. 5a and b, it can be seen that the robot arrives at the end of the reference trajectory and it remains in that position at rest without oscillations. Fig. 5c shows the time evolution of the angles $\theta_n, \theta ref_n$ and θez_n, in a short time interval during the experiment, in order to show properly the difference between the angles $\theta_n, \theta ref_n$ and θez_n. Therein, it can be appreciated how θez approaches θref with the tracking error for the orientation tending to zero.

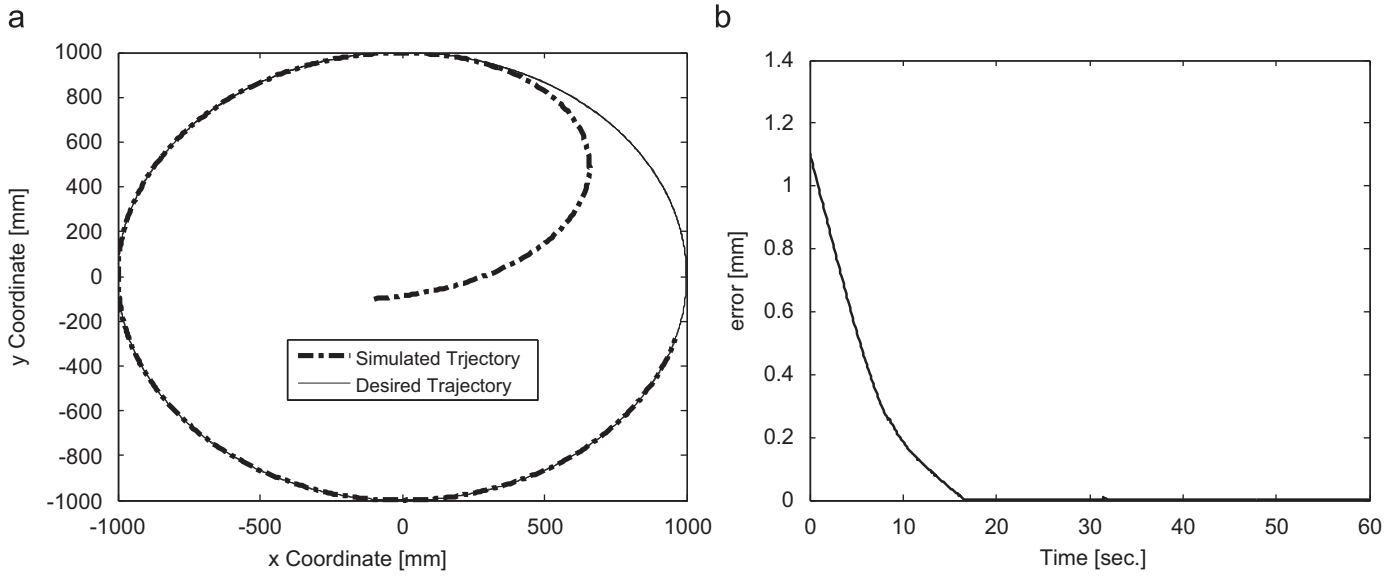

Fig. 3. Simulation results: (a) simulated and desired trajectory; and (b) evolution of error vs time.

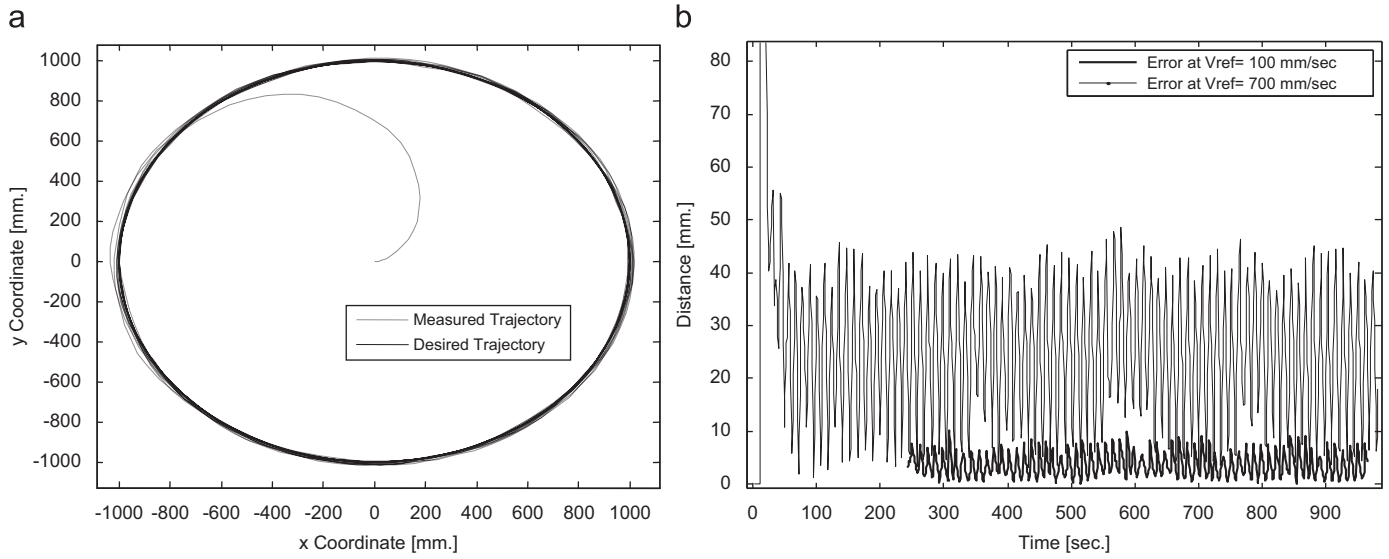

Fig. 4. Experimental results: (a) real and desired trajectory *Vref*=700 mm/s; and (b) error at different reference velocities of 100 and 700 mm/s.

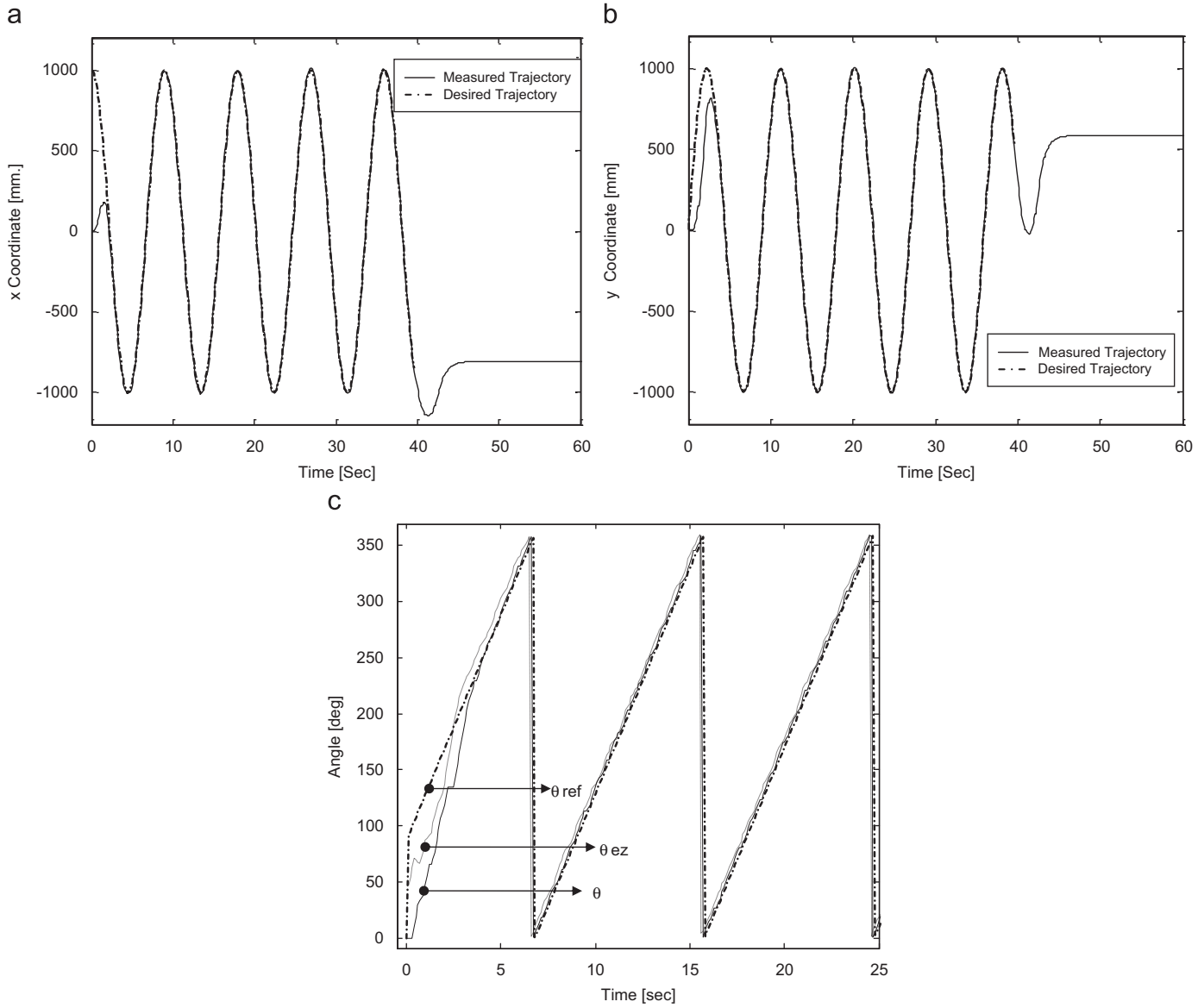

Fig. 5. Experimental results with *Vref*=700 mm/s: (a) time evolution of *x* coordinate; (b) time evolution of *y* coordinate; and (c) time evolution of angles θ_n, θref_n and θez_n.

In Table 1 the maximal errors occurred in the tests for different reference velocities are summarized comparatively. One concludes that the controlled system shows an all-round good performance, even at velocities where the path tracking is much more difficult. This feature illustrates the benefits of the control strategy proposed.

Error analysis: from Eq. (2)

$$|e(x)| \le 0.5 * |(xm-a) * (xm-b)||g''(xm)| = 0.5 * |g''(xm)| * \left|\left(\frac{a+b}{2}-a\right) * \left(\frac{a+b}{2}-b\right)\right|$$

$$|e(x)| \le 0.5 * |g''(xm)| * \left|\left(\frac{b-a}{2}\right) * \left(\frac{a-b}{2}\right)\right| = \frac{1}{8}|g''(xm)| \underbrace{(b-a)^2}_{To}$$

It can be seen that error bound is proportional to the square of sample time and to the second derivative of $g(x)$. Then, by reducing the value of *To* to the half, error bound is reduced by 1/4. In Table 2, the results obtained by simulation are summarized, considering the mobile robot behaviour as Eq. (7) (kinematic ideal model). Errors presented in Table 2 belong to the approach used for different reference velocities and several sample times. It can be seen that if the sample time is reduced in a factor of 1/2, the error is reduced by 4. Nevertheless, the values of the errors are too small compared to the ones obtained in the experimental results with the lab mobile robot (see Table 1). It allows concluding that the main source of error for experimental results presented in Table 1 belongs to unmodelled dynamics of the mobile robot.

Then, in experimental results, by diminishing sample time an error reduction will be observed; this reduction obeys mainly to the fact that the error from unmodelled dynamics is corrected faster, keeping errors from kinematic considerations very small. These results can be seen in Table 3 where errors for different reference velocities and $To = 0.05$ s are shown.

Another important problem issued from the literature (Chwa, 2004) is described as to reach a point in $x-y$ and afterwards to re-orientate the robot in a specified direction established by the trajectory planner. A new experiment that depicts this problem is shown in Fig. 6a, where the mobile robot movement is illustrated step by step. The values for the position and orientation were $xd = 1800$ mm, $yd = 2500$ mm and $\theta d = 170^\circ$. In Fig. 6b the respective evolution of θ_n and θez_n are displayed.

When the positioning error is large, the orientation θez_{n+1} is calculated by using (23). Conversely, when the positioning error and the linear velocity are small then $\theta ez_{n+1} = 170^\circ$ is assumed. It means

$$\theta ez_{n+1} = \begin{cases} a\tan\dfrac{\dfrac{W_n}{V_n}\Delta x + \sin\theta_n}{-\dfrac{W_n}{V_n}\Delta y + \cos\theta_n} & \text{if } \|e_n\| + To|V_n| > \varepsilon \\ 170^\circ & \text{if } \|e_n\| + To|V_n| \le \varepsilon \end{cases} \quad (28)$$

where ε is a value significantly small, for this case the value used was $\varepsilon = 10$ mm. It can be seen from Figs. 6a and b how the mobile robot defines an orientation to reach the point $(x, y) = (1800, 2500)$ mm and when it is close enough to this point, its new desired orientation is $\theta ez_{n+1} = 170^\circ$.

Table 1
Maximum error at different velocities of reference, $To = 0.1$ s.

Vref (mm/s)	100	200	300	400	500	600	700	800
Max. error (mm)	9	16	22	26	33	37	48	54

Table 2
Maximum error at different velocities of reference and different *To*.

VEL *To*	100 mm/s	700 mm/s
0.1 s	2.4693×10^{-2} mm	1.2 mm
0.05 s	5.1536×10^{-3} mm	3.027×10^{-1} mm
	$\frac{2.4693 \times 10^{-2}}{5.1536 \times 10^{-3}} = 4.7914$	$\frac{1.2}{3.027 \times 10^{-1}} = 3.9643$

Table 3
Maximum error at different velocities of reference, $To = 0.05$ s.

Vref (mm/s)	100	200	300	400	500	600	700	800
Max. error (mm)	5	9	14	16	23	26	34	40

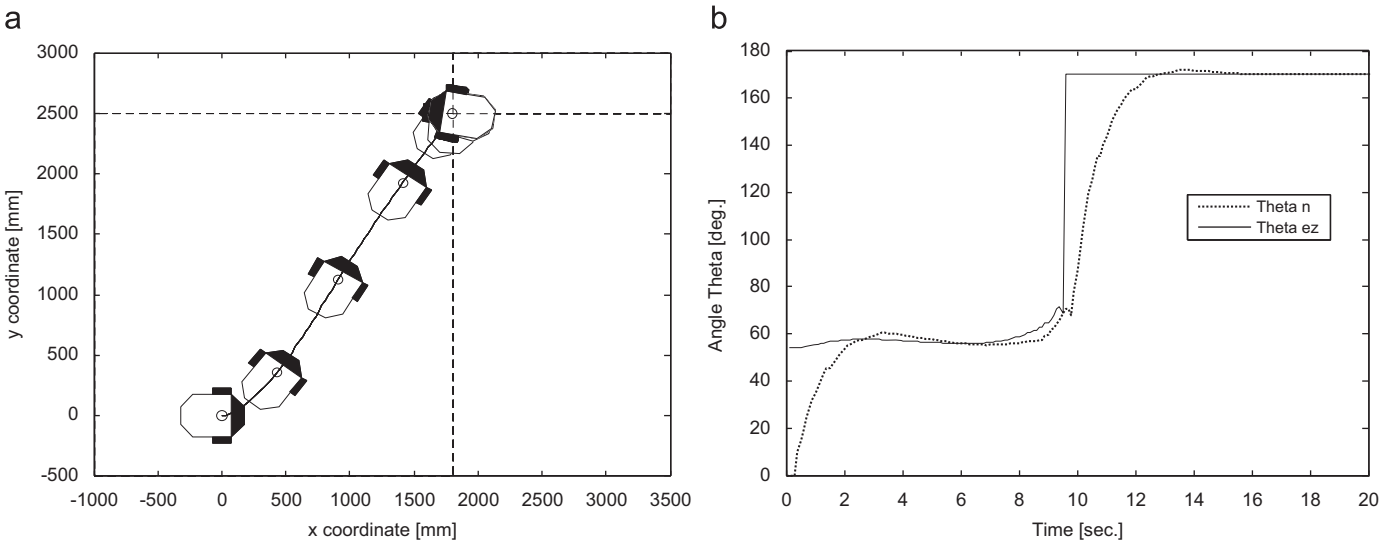

Fig. 6. Experimental results: (a) trajectory followed by PIONEER 2DX in $x-y$ plane; and (b) time evolution of $\theta(t)$.

The speed range used for testing the performance of the proposed controller is typical in the trajectory tracking papers referenced by the current bibliography (Normey-Rico et al., 1999). This fact shows the good performance of the controller.

Finally, the proposed methodology has been tested in a real environment with a PIONEER 2DX mobile robot. A simple case has been tested: the mobile robot must follow a specific pre-established straight trajectory from the position $(-2000, -5000)$ mm until the position $(4750, 3250)$ mm. The mobile robot has not *a-priori* knowledge of this environment, it has no maps or land-marks, therefore PIONEER 2DX must reach its goal avoiding all the obstacles during the tracking. To know its position, the mobile robot uses odometry (Ojeda & Borenstein, 2003).

To map the test-environment, the mobile robot is equipped with a SICK LMS200 laser sensor, which is a sensor that measures distances to surrounding profiles in a two dimensional plane. The laser energy is emitted in a sequence of very short bursts over a maximum scanning angle of 180°. The real test-environment for the PIONEER robot includes doors, boxes, and walls; therefore the mobile robot must avoid collisions during its movement. For a reactive avoidance of obstacles, the field force approach (Rosales, Scaglia, Mut, & di Sciascio, 2009) has been used.

Fig. 7 shows the experimental results that verify the performance of this novel approach. The experimental environment map and the desired trajectory of the mobile robot are presented: thick lines

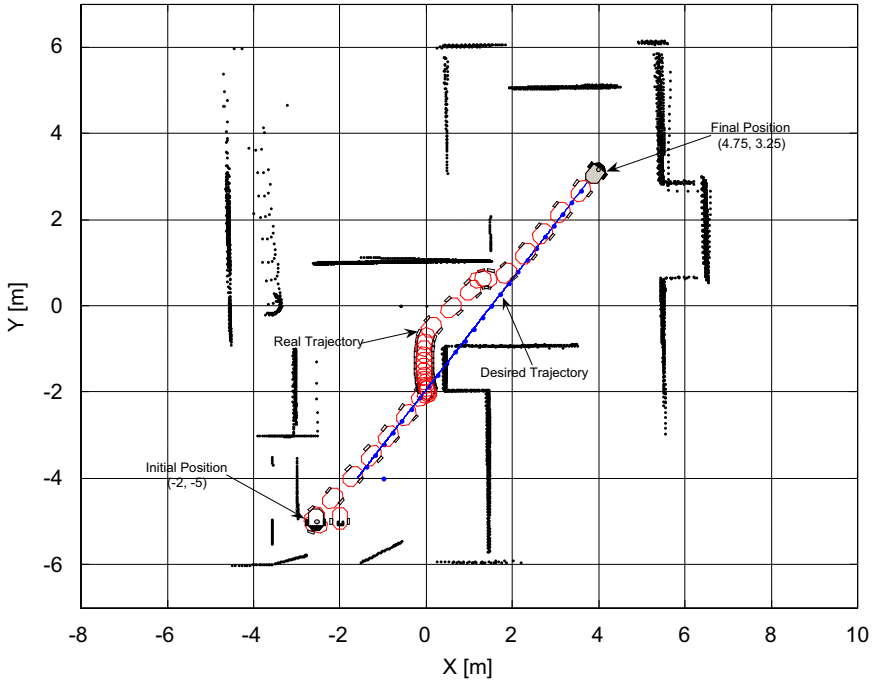

Fig. 7. Experimental results: navigation of PIONEER 2DX in a real environment.

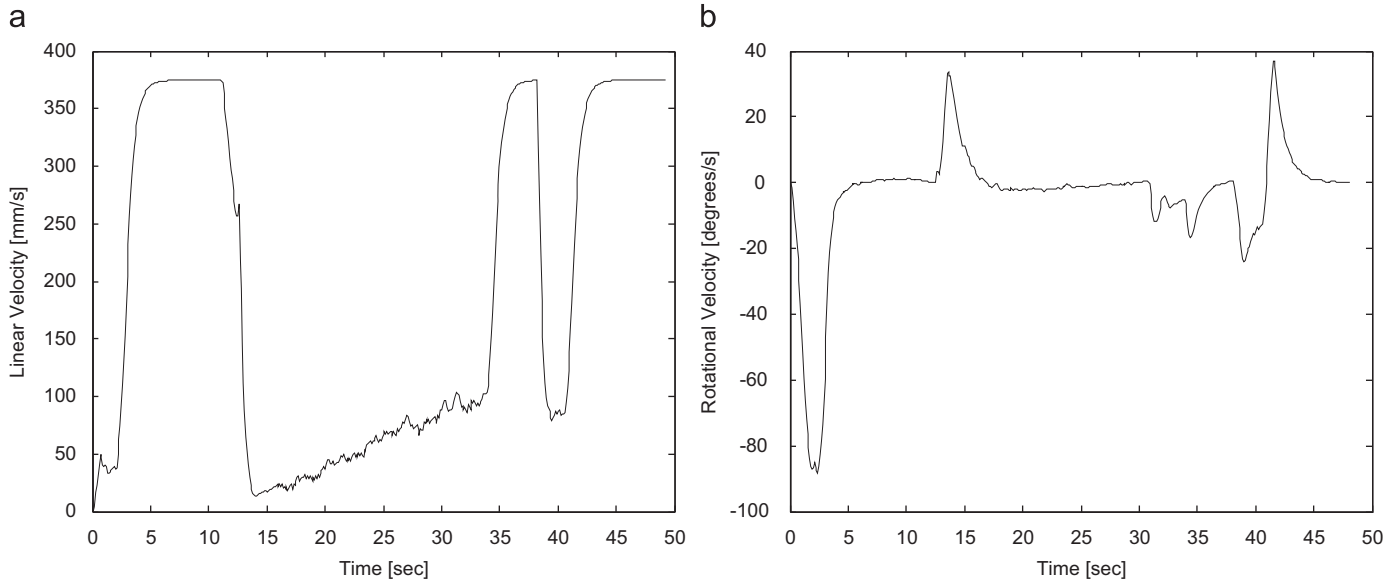

Fig. 8. Experimental results: (a) linear velocity profile; and (b) rotational velocity profile.

correspond to different obstacles detected on-line (walls, boxes, etc.), which are incrementally added into the map, as the mobile robot moves forward. The mobile robot was able to achieve the desired trajectory with a very good performance minimizing the tracking error.

When the mobile robot finds an obstacle, its speed is reduced until the collision has been avoided. The reference trajectory was generated with a constant linear velocity of $Vref$=370 mm/s. Velocity profiles of the last experiment are shown in Fig. 8. Fig. 8a presents the experimental linear velocity of the mobile robot during the real test and Fig. 8b presents the experimental rotational velocity.

One important aspect to clarify the behaviour of the mobile robot during the experiments is that in a trajectory tracking, unlike in a path tracking, the desired point does not wait for the mobile robot, since a trajectory is a time-parameterized path. There are other methods to stop the reference while the mobile robot is approaching (Del Río et al., 2002; Lee & Park, 2003), but in this paper, the most demanding situation has been analysed, because the mobile robot has to reach the reference as soon as possible without colliding with the obstacles. The mobile robot tries to reach the pre-established trajectory while the desired point is moving. The mobile robot's velocity and the trajectory one are on a par, when the desired trajectory is reached by the mobile robot. If an obstacle causes the activation of the collision avoidance strategy, the mobile robot reduces its speed, then the trajectory overtakes the mobile robot, hence when the collision has been already avoided, the mobile robot must accelerate (until its maximum velocity) to reach again the desired trajectory (see Fig. 8). In spite of this challenging assignment, the performance of the mobile robot during the experiments is successful.

It can be observed that the proposed control system is dependent on the precision and accuracy of the sensor system; however, it is independent from the sensor method used. This relies on the fact that not only intern sensors (odometry), but also extern sensors (laser) can be used, depending on the application, complexity or the problem to be solved.

4. Conclusions

A new methodology based on linear interpolation to design control algorithms for trajectory tracking of mobile robots has been presented. For this, the variation of the controlled variables is approximated between two sampling periods, using linear interpolation. Next, by means of algebraic methods, the control signals are computed using a straightforward procedure, which can be used for any robotic platform since only an appropriate model for the robotic system to be controlled will be necessary.

The proposed control strategy has been applied to a nonlinear multivariable system described by a mobile robot. All experiences have shown a good performance for the controlled system, as shown in typical results and laboratory experiences. From the experimental results, we can appreciate that the tracking errors are very low with respect to the mobile robot dimensions. The features of the approach are demonstrated by experiments consisting first in a circular path to be tracked by the vehicle from an outside position at different advance velocities, and secondly the problem of arriving to a specified point and then re-orientating the vehicle to other direction around this point.

To demonstrate the versatility of the proposed methodology, a real navigation case has been tested in an environment with obstacles. In this experiment the mobile robot has perfectly tracked the reference trajectory and avoided the collisions during its movement. Therefore, it can be seen that the combination of this novel technique with collisions avoidance strategies produces a complete controller for the nonholonomic mobile robot navigation. The all-round performance achieved by the controlled system in the experiments is good with small tracking errors.

Acknowledgements

This work was partially funded by the Consejo Nacional de Investigaciones Científicas y Técnicas (CONICET—National Council for Scientific Research), Argentina and the Germany Service for Academic Exchange (DAAD—Deutscher Akademischer Austauschdients).

Appendix A

If the mobile robot behaviour is ruled by (10), (13), (14), and the controller is designed by (26), then, $\|e_n\| \to 0, n \to \infty$ when the positioning ($Vref$=0) and the trajectory tracking ($0 < Vref < \infty$) problems are considered.

From (10), (13) and (14), we have

$$x_{n+1} = x_n + \frac{V_n}{W_n}(\sin\theta_{n+1} - \sin\theta_n) = x_n + V_n To \frac{\sin\theta_{n+1} - \sin\theta_n}{\theta_{n+1} - \theta_n}$$

$$y_{n+1} = y_n + \frac{V_n}{W_n}(\cos\theta_n - \cos\theta_{n+1}) = y_n + V_n To \frac{\cos\theta_n - \cos\theta_{n+1}}{\theta_{n+1} - \theta_n} \tag{A.1}$$

Defining $f(\theta_{n+1})$ and applying Taylor's series

$$f(\theta_{n+1}) = \frac{\sin\theta_{n+1} - \sin\theta_n}{\theta_{n+1} - \theta_n} = f(\theta ez_{n+1}) + \frac{df[\theta ez_{n+1} + \xi(\theta_{n+1} - \theta ez_{n+1})]}{d\theta_{n+1}}(\theta_{n+1} - \theta ez_{n+1}) \tag{A.2}$$

when

$$0 < \xi < 1, \psi = \theta ez_{n+1} + \xi(\theta_{n+1} - \theta ez_{n+1}) \tag{A.3}$$

$$\frac{df}{d\theta_{n+1}} = \frac{\cos\theta_{n+1}(\theta_{n+1} - \theta_n) - (\sin\theta_{n+1} - \sin\theta_n)}{(\theta_{n+1} - \theta_n)^2} \tag{A.4}$$

By replacing (A.2) and (A.3) in (A.1) for x

$$x_{n+1} = x_n + V_n To\left[\frac{\sin\theta ez_{n+1} - \sin\theta_n}{\theta ez_{n+1} - \theta_n} + f'(\psi)(\theta_{n+1} - \theta ez_{n+1})\right] \tag{A.5}$$

From (A.5) and (19) we have

$$V_n To \frac{\sin\theta ez_{n+1}-\sin\theta_n}{\theta ez_{n+1}-\theta_n} = \frac{(\theta ez_{n+1}-\theta_n)}{a^2+b^2}\left[\frac{\Delta x}{To}a+\frac{\Delta y}{To}b\right] To \frac{\sin\theta ez_{n+1}-\sin\theta_n}{\theta ez_{n+1}-\theta_n} = \frac{1}{a^2+b^2}[\Delta x a^2+\Delta y ab] \tag{A.6}$$

$$\Delta x \frac{W_n}{V_n} = \sin\theta ez_{n+1}-\sin\theta_n = a \tag{A.7}$$

$$\Delta y \frac{W_n}{V_n} = \cos\theta_n-\cos\theta ez_{n+1} = b \tag{A.8}$$

$$\frac{\Delta y}{\Delta x} = \frac{b}{a} \Rightarrow \Delta y = \Delta x \frac{b}{a} \tag{A.9}$$

Replacing (A.9) in (A.6)

$$\frac{1}{a^2+b^2}[\Delta x a^2+\Delta y ab] = \frac{1}{a^2+b^2}[\Delta x a^2+\Delta x b^2] = \Delta x$$

And replacing in (A.5)

$$x_{n+1} = x_n+\Delta x+V_n Tof'(\psi)(\theta_{n+1}-\theta ez_{n+1}) \tag{A.10}$$

If (24), is replaced into (A.10)

$$x_{n+1} = xref_{n+1}-kx(xref_n-x_n)+V_n Tof'(\psi)(\theta_{n+1}-\theta ez_{n+1}) \tag{A.11}$$

$ex = xref-x$, then

$$ex_{n+1}-kxex_n+V_n Tof'(\psi)(\theta_{n+1}-\theta ez_{n+1}) = 0 \tag{A.12}$$

Analogous for y, we have $ey = yref-y$

$$y_{n+1} = y_n+V_n To\frac{\cos\theta_n-\cos\theta_{n+1}}{\theta_{n+1}-\theta_n} \tag{A.13}$$

$$g(\theta_{n+1}) = \frac{\cos\theta_n-\cos\theta_{n+1}}{\theta_{n+1}-\theta_n} = g(\theta ez_{n+1})+\frac{dg[\theta ez_{n+1}+\varepsilon(\theta_{n+1}-\theta ez_{n+1})]}{d\theta_{n+1}}(\theta_{n+1}-\theta ez_{n+1}) \tag{A.14}$$

$$0<\varepsilon<1, \psi 1 = \theta ez_{n+1}+\varepsilon(\theta_{n+1}-\theta ez_{n+1}) \tag{A.15}$$

$$ey_{n+1}-kyey_n+V_n Tog'(\psi 1)(\theta_{n+1}-\theta ez_{n+1}) = 0 \tag{A.16}$$

From (15), (16) and (25)

$$\theta_{n+1} = \theta_n+W_n To = \theta ez_{n+1}-k\theta(\theta ez_n-\theta_n) \tag{A.17}$$

$$e\theta_{n+1}-k\theta e\theta_n = 0 \tag{A.18}$$

From (A.12), (A.16) and (A.18),

$$\begin{bmatrix} ex_{n+1} \\ ey_{n+1} \end{bmatrix} = \begin{bmatrix} kx & 0 \\ 0 & ky \end{bmatrix}\begin{bmatrix} ex_n \\ ey_n \end{bmatrix} + \underbrace{\begin{bmatrix} V_n Tof'(\psi) \\ V_n Tog'(\psi 1) \end{bmatrix}\underbrace{(\theta ez_{n+1}-\theta_{n+1})}_{e\theta_{n+1}}}_{Nonlinearity} \tag{A.19}$$

Nonlinearity characterization:

$$V_n = \frac{(\theta ez_{n+1}-\theta_n)}{(\sin\theta ez_{n+1}-\sin\theta_n)^2+(\cos\theta_n-\cos\theta ez_{n+1})^2}\left\{\frac{\Delta x}{To}(\sin\theta ez_{n+1}-\sin\theta_n)+\frac{\Delta y}{To}(\cos\theta_n-\cos\theta ez_{n+1})\right\} \tag{A.20}$$

$$ToV_n = \frac{(\theta ez_{n+1}-\theta_n)}{a^2+b^2}[[xref_{n+1}-kx(xref_n-x_n)-x_n]a+[yref_{n+1}-ky(yref_n-y_n)-y_n]b] \tag{A.21}$$

From (8)

$$xref_{n+1} = xref_n+\int_{nTo}^{(n+1)To} Vref\cos\theta ref\, dt \tag{A.22}$$

$$yref_{n+1} = yref_n+\int_{nTo}^{(n+1)To} Vref\sin\theta ref\, dt \tag{A.23}$$

$$ToV_n = \frac{(\theta ez_{n+1}-\theta_n)}{a^2+b^2}\left\{\left[xref_n+\int_{nTo}^{(n+1)To} Vref\cos\theta ref\, dt-kx(xref_n-x_n)-x_n\right]a+\left[yref_n+\int_{nTo}^{(n+1)To} Vref\sin\theta ref\, dt-ky(yref_n-y_n)-y_n\right]b\right\} \tag{A.24}$$

$$ToV_n = \frac{(\theta ez_{n+1}-\theta_n)}{a^2+b^2}\left\{\left[\int_{nTo}^{(n+1)To} Vref\cos\theta ref\,dt+(1-kx)(xref_n-x_n)\right]a+\left[\int_{nTo}^{(n+1)To} Vref\sin\theta ref\,dt+(1-ky)(yref_n-y_n)\right]b\right\} \tag{A.25}$$

$$ToV_n = \frac{(\theta ez_{n+1}-\theta_n)}{a^2+b^2}\left\{\left[(1-kx)a\ \ (1-ky)b\right]\begin{bmatrix}ex_n\\ey_n\end{bmatrix}+b\int_{nTo}^{(n+1)To} Vref\sin\theta ref\,dt+a\int_{nTo}^{(n+1)To} Vref\cos\theta ref\,dt\right\} \tag{A.26}$$

If is multiplied and divided by $(\theta ez_{n+1}-\theta_n)$, then

$$ToV_n = \frac{1}{\dfrac{a^2+b^2}{(\theta ez_{n+1}-\theta_n)^2}}\left\{\left[(1-kx)\frac{a}{(\theta ez_{n+1}-\theta_n)}\quad(1-ky)\frac{b}{(\theta ez_{n+1}-\theta_n)}\right]\begin{bmatrix}ex_n\\ey_n\end{bmatrix}++\frac{b}{(\theta ez_{n+1}-\theta_n)}\int_{nTo}^{(n+1)To} Vref\sin\theta ref\,dt\right.$$
$$\left.+\frac{a}{(\theta ez_{n+1}-\theta_n)}\int_{nTo}^{(n+1)To} Vref\cos\theta ref\,dt\right\} \tag{A.27}$$

$$\lim_{(\theta ez_{n+1}-\theta_n)\to 0}\frac{a}{(\theta ez_{n+1}-\theta_n)}=\cos\theta_n,\ \lim_{(\theta ez_{n+1}-\theta_n)\to 0}\frac{b}{(\theta ez_{n+1}-\theta_n)}=\sin\theta_n\Rightarrow\lim_{(\theta ez_{n+1}-\theta_n)\to 0}\frac{a^2+b^2}{(\theta ez_{n+1}-\theta_n)^2}=1$$

Then, the term ToV_n is bounded:

$$\lim_{(\psi-\theta_n)\to 0} f'(\psi)=\lim_{(\psi-\theta_n)\to 0}\frac{\cos\psi(\psi-\theta_n)-(\sin\psi-\sin\theta_n)}{(\psi-\theta_n)^2} \tag{A.28}$$

$$=\lim_{(\psi-\theta_n)\to 0}\frac{\cos\psi}{(\psi-\theta_n)}-\lim_{(\psi-\theta_n)\to 0}\frac{(\sin\psi-\sin\theta_n)}{(\psi-\theta_n)}\frac{1}{(\psi-\theta_n)}\to 0 \tag{A.29}$$

Next $V_nTof'(\psi)$ is bounded, similarly it can be probed that $V_nTog'(\psi)$ is bounded. Besides, it can be seen from (A.18) as the term $(\theta ez_{n+1}-\theta_{n+1})\to 0$ then the nonlinearity is bounded and tends to zero.

If positioning problem is considered, the value of $Vref=0$. Then, by using Agarwal (2000) (Theorem 5.3.1, Chapter 5, p. 248) is fulfilled that $\|e_n\|\to 0$ with $n\to\infty$.

If the trajectory tracking problem with $Vref\neq 0$ is considered, then $\|e_n\|\to 0$ with $n\to\infty$. From (A.19)

$$\begin{bmatrix}V_nTof'(\psi)\\V_nTog'(\psi 1)\end{bmatrix}=\begin{bmatrix}f'(\psi)\dfrac{(\theta ez_{n+1}-\theta_n)}{a^2+b^2}\left\{[(1-kx)a\ \ (1-ky)b]\begin{bmatrix}ex_n\\ey_n\end{bmatrix}+b\int_{nTo}^{(n+1)To} Vref\sin\theta ref\,dt+a\int_{nTo}^{(n+1)To} Vref\cos\theta ref\,dt\right\}\\ g'(\psi 1)\dfrac{(\theta ez_{n+1}-\theta_n)}{a^2+b^2}\left\{[(1-kx)a\ \ (1-ky)b]\begin{bmatrix}ex_n\\ey_n\end{bmatrix}+b\int_{nTo}^{(n+1)To} Vref\sin\theta ref\,dt+a\int_{nTo}^{(n+1)To} Vref\cos\theta ref\,dt\right\}\end{bmatrix} \tag{A.30}$$

then (A.19) can be written as

$$v_{n+1}=\mathbf{A}v_n+\mathbf{B}_nv_n+\mathbf{P}_n \tag{A.31}$$

where

$$v_n=\begin{bmatrix}ex_n\\ey_n\end{bmatrix},\mathbf{A}=\begin{bmatrix}kx & 0\\0 & ky\end{bmatrix} \tag{A.32}$$

$$\mathbf{B}_n=\begin{bmatrix}f'(\psi)\dfrac{(\theta ez_{n+1}-\theta_n)}{a^2+b^2}(1-kx)a & f'(\psi)\dfrac{(\theta ez_{n+1}-\theta_n)}{a^2+b^2}(1-ky)b\\ g'(\psi 1)\dfrac{(\theta ez_{n+1}-\theta_n)}{a^2+b^2}(1-kx)a & g'(\psi 1)\dfrac{(\theta ez_{n+1}-\theta_n)}{a^2+b^2}(1-ky)b\end{bmatrix}e\theta_{n+1} \tag{A.33}$$

$$\mathbf{P}_n=\frac{(\theta ez_{n+1}-\theta_n)}{a^2+b^2}\left(b\int_{nTo}^{(n+1)To} Vref\sin\theta ref\,dt+a\int_{nTo}^{(n+1)To} Vref\cos\theta ref\,dt\right)\begin{bmatrix}f'(\psi)\\g'(\psi 1)\end{bmatrix}e\theta_{n+1}=\begin{bmatrix}P_{1n}\\P_{2n}\end{bmatrix}e\theta_{n+1} \tag{A.34}$$

where $\mathbf{B}_n$ and $\mathbf{P}_n$ are limited, and moreover it is true that $\mathbf{B}_n,\mathbf{P}_n\to 0\ \ n\to\infty$, due to $\lim_{n\to\infty}e\theta_n=0$.

$$v_n=\mathbf{A}^nv_0+\sum_{l=1}^{n}\mathbf{A}^{n-l}[\mathbf{B}_{l-1}v_{l-1}+\mathbf{P}_{l-1}] \tag{A.35}$$

$$v_n=\mathbf{A}^nv_0+\sum_{l=1}^{n}\mathbf{A}^{n-l}\mathbf{B}_{l-1}v_{l-1}+\sum_{l=1}^{n}\mathbf{A}^{n-l}\mathbf{P}_{l-1} \tag{A.36}$$

$$\|v_n\|\leq\left\|\mathbf{A}^nv_0+\sum_{l=1}^{n}\mathbf{A}^{n-l}\mathbf{B}_{l-1}v_{l-1}\right\|+\left\|\sum_{l=1}^{n}\mathbf{A}^{n-l}\mathbf{P}_{l-1}\right\| \tag{A.37}$$

$$\|v_n\|\leq c0[\delta(1+c2)]^{n-k1}+\left\|\sum_{l=1}^{n}\mathbf{A}^{n-l}\mathbf{P}_{l-1}\right\| \tag{A.38}$$

$$\| \sum_{l=1}^{n} \mathbf{A}^{n-l}\mathbf{P}_{l-1} \| \leq \max\sqrt{(\mathbf{P}_{1n}^2+\mathbf{P}_{2n}^2)}|e\theta_0| \| \sum_{l=1}^{n} \mathbf{A}^{n-l}k\theta^{l-1} \| \tag{A.39}$$

where $e\theta_0$ is the initial angle error and $0 < k\theta < 1$.

We can always choose $\delta(1+c2) < 1$, (Agarwal, 2000 (Theorem 5.2.3, pp. 240–241)), applying Toeplitz Lemma, (Agarwal, 2000, pp. 682), it is true that

$$\lim_{n\to\infty} \sum_{l=1}^{n} \mathbf{A}^{n-l}k\theta^{l-1} = 0 \tag{A.40}$$

then from (A.38), (A.39), (A.40)

$$\lim_{n\to\infty} \|v_n\| = 0 \tag{A.41}$$

Appendix B. Supplementary materials

Supplementary data associated with this article can be found in the online version at 10.1016/j.conengprac.2009.11.011.

References

Agarwal, R. (2000). *Difference equations and inequalities, theory, methods, and applications*. New York: Marcel Dekker.

Campion, G., Bastin, G., & d'Andrea-Novel, B. (1996). Structural properties and classification of kinematic and dynamic models of wheeled mobile robots. *IEEE Transaction on Robotics and Automation*, *12*(1), 47–62.

Chwa, D. (2004). Sliding-mode tracking control of nonholonomic wheeled mobile robots in polar coordinates. *IEEE Transactions on Control Systems Technology*, *12*(4).

Cruz, D., Mcclintock, J., Perteet, B., Orqueda, O. A.A., Cao, Y., & Fierro, R. (2007). Decentralized cooperative control—a multivehicle platform for research in networked embedded systems. *Control Systems Magazine IEEE*, *27*(3), 58–78.

Del Rio, F., Jiménez, G., Sevillano, J., Amaya, C., & Balcells, A. (2002). Error adaptive tracking for mobile robots. In *Proceedings of the annual conference on IEEE industrial electronics society*, *2002* (pp. 2415-2420).

Do, K. D., & Pan, J. (2006). Global output-feedback path tracking of unicycle-type mobile robots. *Robotics and Computer-Integrated Manufacturing*, *22*, 166–179.

Dong, W., & Guo, Y. (2005). Dynamic tracking control of uncertain mobile robots. *IEEE/RSJ International Conference on Intelligent Robots and Systems*, 2774–2779.

Fierro, R., & Lewis, F. (1995). Control of a nonholonomic mobile robot: Backstepping kinematics into dynamics. In *Proceedings of the 34th conference on decision & control* (Vol. 4, pp. 3805–3810), New Orleans, LA—December 1995.

Fukao, T., Nakagawa, H., & Adachi, N. (2000). Adaptive tracking control of a nonholonomic mobile robot. *IEEE Transactions on Robotics and Automation*, *16*(5), 609–615.

Kanayama, Y., Kimura, Y., Miyazaki, F., & Noguchi, T. (1990). A stable tracking control method for an autonomous mobile robot. In *Proceedings of the IEEE international conference on robotics and automation* (pp. 384–389).

Kim, S., Shin, J., & Lee, J. (2000). Design of a robust adaptive controller for a mobile robot. In *Proceedings of 2000 IEEE/RSJ international conference on intelligent robots and systems* (Vol. 3, pp. 1816–1821).

Klanèar, G., & Škrjank, I. (2007). Tracking-error model-based predictive control for mobile robots in real time. *Robotics and Autonomous Systems*, 460–469.

Lee, S., & Park, J. H. (2003). Virtual trajectory in tracking control of mobile robots. In *Proceedings of the 2003 IEEE/ASME international conference on advanced intelligent mechatronic (AIM 2003)*.

Lee, T., Song, K., Lee, C., & Teng, C. (2001). Tracking control of unicicle-modeled mobile robots using a saturation feedback controller. *IEEE Transactions on Control Systems Technology*, *9*(2).

Liu, Z. Y., Jing, R. H., Ding, X. Q., & Li, J. H. (2008). Trajectory tracking control of wheeled mobile robots based on the artificial potential field. In *Fourth international conference on natural computation* (pp. 382–387).

Liu, S., Zhang, H., Yang, S. X., & Yu, J. (2004). Dynamic control of a mobile robot using an adaptive neurodynamics and sliding mode strategy. In *Proceedings of the fifth congress intelligent control and automation* (pp. 5007–5011).

Martins, F., Celeste, W., Carelli, R., Sarcinelli-Filho, M., & Bastos-Filho, T. (2008). An adaptive dynamic controller for autonomous mobile robot trajectory tracking. *Control Engineering Practice*, *16*, 1354–1363.

Normey-Rico, J., Gomez-Ortega, J., & Camacho, E. (1999). A Smith-predictor-based generalized predictive controller for mobile robot path-tracking. *Control Engineering Practice*, *7*, 729–740.

Ojeda, L., & Borenstein, J. (2003). Reduction of odometry errors in over-constrained mobile robots. In *Proceedings of the UGV technology conference at the SPIE aerosense symposium*.

Rosales, A., Scaglia, G., Mut, V., & di Sciascio, F. (2009). *Trajectory tracking of mobile robots in dynamic environments—A linear algebra approach, ROBOTICA*. Cambridge: Cambridge University Press10.1017/S0263574709005402.

Scaglia, G., Quintero, L., Mut, V., & di Sciascio, F. (2008). Numerical methods based controller design for mobile robots. In *Proceedings of the 17th world congress the international federation of automatic contro*l (IFAC) (pp. 4820–4827), Seoul, Korea, July 6–11.

Secchi, H. (1998). *Control of autoguided vehicle with sensorial feedback*. Master thesis (in spanish). Edit Fundación Universidad Nacional de San Juan, ISBN 950-605-190-9, San Juan, Argentina.

Shim, H., & Sung, Y. (2004). Stability and four-posture control for nonholonomic mobile robots. *IEEE Transactions on Robotics and Automation*, *20*(1).

Strang, G. (1980). *Linear algebra and its applications*. New York: Academic Press.

Sun, S. (2005). Designing approach on trajectory—tracking control of mobile robot. *Robotics and Computer-Integrated Manufacturing*, *21*(1), 81–85.

Sun, S., & Cui, P. (2004). Path tracking and a practical point stabilization of mobile robot. *Robotics and Computer-Integrated Manufacturing*, *20*, 29–34.

Tsai, P. S., Wang, L. S., Chang, F. R., & Wu, T. F. (2004). Systematic backstepping design for B-spline trajectory tracking control of the mobile robot in hierarchical model. In *International conference on networking, sensing and control* (pp. 713–718).

Tsuji, T., Morasso, P., & Kaneko, M. (1995). Feedback control of nonholonomic mobile robots using time base generator. *In Proceedings of IEEE international conference on robotics and automation* (Vol. 2, pp. 1385–1390), Nagoya Japan.

Vougioukas, S. (2007). Reactive trajectory tracking for mobile robots based on non linear model predictive control. In *International conference on robotics and automation* (pp. 3074–3079).

Wang, T. Y., & Tsai, C. C. (2004). Adaptive trajectory tracking control of a wheeled mobile robot via Lyapunov techniques. In *Annual conference of IEEE industrial electronics society* (pp. 389–394).

Zhang H. -X., Dai G. -J., & Zeng H. (2007). A trajectory tracking control method for nonholonomic mobile robots. In *International conference on wavelet analysis and pattern recognition* (pp. 7–11).